Multipoint laser Doppler vibrometry with single detector : principles, implementations, and signal analyses

Fu, Yu; Guo, Min; Phua, Poh Boon

2011

Fu, Y., Guo, M. & Phua, P. B. (2011). Multipoint laser Doppler vibrometry with single detector: principles, implementations, and signal analyses. Applied Optics, 50(10), 1280-1288.

https://hdl.handle.net/10356/92566

https://doi.org/10.1364/AO.50.001280

Multipoint laser Doppler vibrometry with single detector: principles, implementations, and signal analyses

Y. Fu,[1] M. Guo,[1] and P. B. Phua[1,2,*]

[1]Temasek Laboratories & School of Physical and Mathematical Sciences, Nanyang Technological University, 50 Nanyang Drive, Singapore 637553

[2]DSO National Laboratories, 20 Science Park Drive, Singapore 118230

*Corresponding author: ppohboon@alum.mit.edu

Received 19 November 2010; revised 20 January 2011; accepted 25 January 2011; posted 26 January 2011 (Doc. ID 138431); published 23 March 2011

A 20-point laser Doppler vibrometer with single photodetector is presented for noncontact dynamic measurement. A 5×4 beam array with various frequency shifts is generated by a $1.55\,\mu$m distributed feedback laser and four acousto-optic devices, and illuminating different points on vibrating objects. The reflected beams are coupled into a single-mode fiber by a pigtailed collimator and interfere with a reference beam. The signal output from a high-speed photodetector is amplified and then digitized by a high-speed analog-to-digital converter with a sampling rate of 1 gigasample per second (1 GS/s). Several methods are introduced to avoid the cross talk among different frequencies and extract the vibration information of 20 points from a one-dimensional signal. Two signal processing algorithms based on Fourier transform and windowed Fourier transform are illustrated to extract the vibration signals at different points. The experimental results are compared with that from a commercial single-point laser vibrometer. The results show simultaneous vibration measurement can be realized on multiple points using a single laser source and a single photodetector.

OCIS codes: 120.7280, 120.3180, 120.4290, 070.1060.

1. Introduction

Optical interferometry has been applied on dynamic measurement for many years. Generally there are two types of techniques: (1) camera-based optical interferometry and (2) photodetector-based laser Doppler vibrometry. Both techniques enjoy the virtues of being noncontact and high accuracy, and have gained ground in many engineering applications. In 1990s, the imaging rate of cameras was very low. Hence, optical dynamic measurements based on the time-averaged method [1] or the usage of stroboscopic [2] or double-pulsed [3] coherent light sources are still static or quasi-static technologies. With the availability of high-speed cameras, it is now possible to record interferograms with rates exceeding 100,000 frames per second. Temporal [4,5] and spatiotemporal [6,7] analyses of the recorded interferogram sequence lead to full-field measurement of the instantaneous kinematic and deformation parameters of a testing object. However, because of the constraint of the Nyquist sampling theorem, the velocity measurement range of camera-based techniques is still very low.

On the other hand, photodetector-based laser Doppler vibrometry (LDV) [8] can only offer a pointwise measurement, but with much larger measurement ranges on vibration amplitude and frequency; in other words, a larger measurement range on velocity. The LDV is based on the Doppler effect that occurs when the laser light scatters from a moving surface. The instantaneous velocity of the surface is converted to the Doppler frequency shift of the laser light, which can be extracted by interference between

0003-6935/11/101280-09$15.00/0

the object and reference beams. To avoid the directional ambiguity problem, the heterodyne, as a Mach–Zehnder interferometer (including one detector and one acousto-optic modulator), and the homodyne, as Michelson interferometer, (including two detectors and polarization components) are two typical configurations of LDVs. Most of the vibrometric systems offer pointwise measurement; this becomes a main disadvantage of LDVs. To measure vibration at different points, a scanning system containing two orthogonal mirrors is normally adopted to move the measurement point rapidly and precisely on the testing surface [9]. This approach assumes that the measurement conditions remain invariant while sequential measurements are performed. Hence, it is only suitable for measuring steady-state or well-characterized vibrations. However, most engineering applications do not satisfy these requirements. Transients, including impact or coupled vibrations, are commonly observed in real applications. This makes scanning LDVs impractical for generating a vibration image in these cases.

In recent years, several types of multichannel and multipoint LDVs have been reported [10,11] by different research groups. This novel idea first appeared in a scientific paper in which Zheng *et al.* [12] proposed a multichannel laser vibrometer based on a commercial single-point Polytec vibrometer and an acousto-optic beam multiplexer. It is still a pointwise measurement, but with a switch among different channels instead of a scanning mechanism. Now some robust prototypes [13] and even customer-designed commercial products [14] can be found. However, these multibeam versions are normally a combination of several sets of single-point vibrometers [15], or use multiple detectors or detector arrays [10,11,13–16], which still need synchronization. Recently, some simultaneous multipoint measurements [17–19] using one laser source and one detector have been reported in the akin technique of laser Doppler velocimetry, which has widely been used in experimental fluid mechanics for flow measurement. These techniques use at least two acousto-optic devices to generate various frequency shifts at spatially separated points, and resolve the signals in the frequency domain. However, the results presented are limited in the measurement to two or three points, where the cross-talk region can be easily separated in the spectrum. The same approach suffers when it is applied in LDV, as all object beams will interfere with a common reference beam, and the object beams will also interfere with each other. Resolving the measurement signals from the cross-talk region is difficult when the number of measurement points is increasing.

In our previous publication [20], we proposed a new method of generating a 2×5 beam array with different frequency shifts, and realized a simultaneous vibration measurement on 10 points using a single photodetector. In this paper, we expand the technique to a 20-point measurement. A 5×4 beam array with various frequency shifts is generated by a $1.55\,\mu$m distributed feedback (DFB) laser and four acousto-optic devices, and illuminating different points of two vibrating cantilever beams. The reflected beams are collected by a pigtailed collimator and interfere with a reference beam. The signal output from a high-speed photodetector is amplified and then digitized by a high-speed analog-to-digital (A–D) converter with a sampling rate of 1 gigasample per second (1 GS/s). Several methods to avoid the cross talk among 20 object beams in the experimental and signal processing stages are discussed. Two signal processing algorithms, based on Fourier analysis and windowed Fourier analysis, are compared in the processing of a one-dimensional (1-D) interference signal. Simultaneous measurement of velocity and displacement is realized on 20 different points. In addition, the results are compared with that from a Polytec single-point laser Doppler vibrometer. The comparison shows the advantages and potential of applying the spatially encoded LDV concept for multipoint vibration measurement using a single photodetector.

2. Theoretical Analysis

A. Doppler Shift and Single-Point Heterodyne Interferometer with an Acousto-Optic Modulator

In a single-beam LDV, a laser beam with wavelength of λ is projected on an object moving with velocity $\boldsymbol{V}$; the shifted frequency f_D of the reflected laser beam is proportional to the velocity of the object due to the Doppler effect and can be expressed as

$$f_D(t) = \frac{V(t) \cdot \mathbf{S}}{\lambda}, \tag{1}$$

where $\mathbf{S} = \mathbf{e}_i - \mathbf{e}_o$ is the sensitivity vector given by the geometry of the setup, and $\mathbf{e}_i$ and $\mathbf{e}_o$ are the unit vectors of illumination and observation, respectively. $\mathbf{S}$ can be considered as 2 when the illumination and observation are approximately at a right angle. In order to avoid the directional ambiguity in a frequency shift, the most common solution is the heterodyne interferometer, where an optical frequency shift is introduced into one arm of the interferometer by an acousto-optic modulator (AOM) to obtain a virtual velocity offset. The intensity fluctuation at the detector can be expressed as [21]

$$I = I_{\mathrm{DC}} + I_{\mathrm{RO}} \cos(2\pi(f_D + f_{\mathrm{AOM}})t + \Delta\phi), \tag{2}$$

where f_D and f_{AOM} are the Doppler frequency shift and the carrier frequency introduced by the AOM, respectively. $\Delta\phi$ is the phase difference between the reference beam and the object beam. The modulation factor I_{RO} is determined by $\sqrt{I_R I_O}$, the product of the square root of the object and reference beam intensities. A photodetector will convert the intensity fluctuation to a current signal for later analog or digital decoding.

B. Multibeam Laser Doppler Vibrometer

In this paper, we propose a spatially encoded 20-beam laser Doppler vibrometer. Twenty laser beams with different frequency shifts are projected onto a vibrating object. The reflected beam array is collected by a pigtailed collimator, and interferes with a reference beam.

The detected interference signal can be expressed by

$$\begin{aligned} I =& I_{\mathrm{DC}} + \sum_{i=1}^{20} I_{M(i)} \cos(2\pi(f_{D(i)} + f_{\mathrm{AOM}(i)})t + \Delta\phi_{(i)}) \\ &+ \sum_{m=1}^{19} \sum_{n>m}^{20} I_{mn} \cos(2\pi[(f_{D(m)} - f_{D(n)}) \\ &+ (f_{\mathrm{AOM}(m)} - f_{\mathrm{AOM}(n)})]t + \Delta\phi_{mn}), \end{aligned} \tag{3}$$

where $i = 1, 2, \ldots 20$, m and n are integers, and $f_{\mathrm{AOM}(i)}$ are the central frequencies of the 20 object beams; The second term is the interference signal between 20 object beams and the reference beam, from which the useful vibration information of 20 points can be extracted. The third term is the sum of the cross talk between any two object beams, which has to be avoided when the interference signal is decoded. In order to extract the vibration information of 20 points from the second term, the central frequencies of the laser beams have to be elaborately designed so that the useful signals can be separated from cross-talk regions in the frequency spectrum or the temporal-frequency spectrogram. Once it is achieved, it is possible to extract the vibration information of 20 points from a single 1-D signal using the following algorithms.

C. Signal Processing Algorithms for a Long 1-D Signal

Generally, there are two typical demodulation methods in an LDV system, analog demodulation and digital demodulation. The former method normally demodulates the analog input signal by use of the phase-locked-loop technique, and the output is still an analog signal whose voltage variation is proportional to the velocity of the measurement point. In this application, a new technology, digital demodulation, is proposed to decode the 1-D signal by different processing algorithms.

In digital demodulation, a high-speed A–D converter is used to digitize the interference signal. Because of the high carrier frequencies of laser beams, the sampling rate should be high enough (1 GS/s in this application) to satisfy the Nyquist theorem. Hence, a long signal is obtained when a high-frequency resolution is required. Two signal processing algorithms, Fourier analysis [22] and the windowed Fourier ridge method [23], are proposed to obtain the velocity and displacement at different points from a 1-D signal. The details of Fourier analysis and the windowed Fourier Ridge method can be found in Ref. [7]. However, it is worth addressing the following points for these two algorithms.

1. *Fourier Analysis*

1. In Fourier analysis, the digitized signal is first transformed, and one side of the spectrum is filtered with different bandpass filters that are designed according to the carrier frequencies of the AOM and the velocity measurement range. The filtered spectrums are inverse transformed to obtain the wrapped phase at each frequency band. The phase values are then unwrapped along the time axis to obtain the displacements at different frequency bands; in other words, at different points.
2. For a long 1-D signal, it is difficult to process the whole length by a normal computer. Hence, it is necessary to split the signal into several parts and process separately. A continuous displacement can still be obtained by connecting the separated results together.
3. It is well known that the accuracy of Fourier analysis increases when the bandpass filter is narrow. However, the bandpass filter in LDV is determined by the velocity measurement range. The wider the filter, the more serious the noise. It will affect the results in both analog and digital demodulation systems in this application.

2. *Windowed Fourier Ridge*

1. A windowed Fourier ridge (WFR) method maps a 1-D temporal signal to a two-dimensional (2-D) time-frequency plane and extracts the signal's instantaneous frequency with the highest energy. Thus, it is more effective at removing the noise within the selected frequency band. This is the advantage of the WFR technique over Fourier analysis.
2. When a useful signal is mixed with cross-talk signals at a certain frequency band, it is still possible to extract the instantaneous frequency of the useful signal with WFR when its energy is much higher than the mixed cross-talk signals. In this application, it could tremendously increase the measurement range when $I_{M(i)}$ is much larger than $\sum_{m=1}^{19} \sum_{n>m}^{20} I_{mn}$ in Eq. (3). Examples will be shown in Subsection 3.B.3.
3. As WFR includes a frequency scan, it requires a longer processing time compared to Fourier analysis. However, for a 1-D long signal obtained by a digital LDV, it is not necessary to process each sampling point on the time axis. Because WFR can extract the instantaneous frequency (velocity) at any point along the time axis, it is reasonable to process sampling points with a certain time interval. Instantaneous displacement can be obtained by a numerical integration. Hence, the phase unwrapping along the time axis is avoided. This will dramatically reduce the processing time. However, when the displacement is extracted by integration, it is possible to generate an accumulated error. This accumulated error may generate a DC offset when transient

displacement is measured, but it can be easily removed when vibration is the only concern.

4. The wavelet ridge detection algorithm is almost the same as WFR, but the processing window size varies automatically according to the frequency of the signal [22]. This is an advantage over the WFR in many cases when the frequency of the signal is varying dramatically. However, in this application, the frequency fluctuations are not obvious compared to the virtual frequency shift by AOMs. Hence, WFR is still selected to process the signal at different frequency bands. Sometimes it is more practical to avoid some unexpected errors generated by wavelet analysis when the window size varies automatically [7].

3. Design and Generation of a Spatially Encoded Beam Array

In the proposed spatially encoded laser Doppler vibrometer, a beam array with different carrier frequencies is generated and projected on different points of a vibrating specimen. Obviously, it is not reasonable to use one AOM for each channel. Hence, a combination of different types of AOMs in the Bragg and Raman–Nath regimes with some optical components is proposed to generate a beam array cost effectively.

A. Assembly of AOMs in the Raman–Nath and Bragg Regimes

Light diffracted by an acoustic wave of a single frequency produces two distinct diffraction types, Raman–Nath diffraction and Bragg diffraction [24]. In the Raman–Nath regime, several diffracted waves are produced, but the phenomenon is only observed with relatively low acoustic frequencies. In this study, only five orders (−2, −1, 0, +1, +2 orders) with nonuniform intensities (1.0∶9.0∶5.0∶9.0∶1.0) are observed when a 20 MHz frequency is applied. In the Bragg regime, essentially only one diffracted wave is produced. It occurs at higher acoustic frequencies. By a variable rf drive power, the intensity of two output beams at the 0 and +1 orders can be uniform. In this application, we use four different AOMs to generate a 5 × 4 beam array with a frequency interval of 20 MHz: (1) a pigtailed AOM with a 50 MHz frequency shift (Brimrose, AMF-50-1550-2FP+); (2) a pigtailed AOM with a 250 MHz frequency shift (Brimrose, TEF-250-1550-2FP); (3) a frequency shifter in the Bragg regime (Brimrose, AMF-100-1550, separation angle = 62 mrad, rf power tunable, aperture 2 mm × 5 mm), which can generate a two-beam array of the 0 and +1 diffraction orders in x direction with a frequency shift of $f_{\mathrm{Bragg}} = 100$ MHz [Fig. 1(a)]; and (4) a frequency shifter in the Raman–Nath regime (Brimrose, AMF-20-1550, separation angle = 12 mrad, rf power tunable, aperture 2 mm), it can generate a beam array of five diffraction orders (−2, −1, 0, +1, +2) in the y direction with a frequency shift of $f_{\mathrm{RN}} = 20$ MHz in between [Fig. 1(b)]. Figure 2(a) shows the experimental setup of the proposed 20-point laser Doppler vibrometer. A laser beam from a DFB laser system is split into a reference beam and an object beam by a 1∶99 single-mode-fiber coupler. The object beam is then split into two by a 20∶80 single-mode-fiber coupler, and then connected to pigtailed AOMs with 50 and 250 MHz, respectively. As the power losses of these two AOMs are different, the ratio of the fiber coupler is selected to balance the output power. Then two laser beams are collimated by two gradient-index (GRIN) lenses, which are adjusted precisely to form a pair of parallel beams. Figure 1(c) shows the frequency shifts of these two laser beams at position I in Fig. 2(a). The distance between these two beams is restricted by the aperture of the Bragg frequency shifter in the x direction, in this case, <5 mm. Two +1 order beams output from the Bragg frequency shifter are reflected by two mirrors and form a parallel beam array [shown in Fig. 1(d)] in the x direction together with two zero-order beams at position II in Fig. 2(a). Each beam generates a five-beam array in the y direction by the frequency shifter in Raman–Nath regime. Hence. a 5 × 4 array with frequency shifts from 10 to 390 MHz with 20 MHz intervals can be observed. Figure 1(e) shows the distribution of frequency shift of this array at position III in Fig. 2(a). Figure 1(f) shows the intensity distribution on an infrared sensing card. The beam array is projected on a vibrating object and the reflected beams are collected by a pigtailed collimator and interfere with the reference beam.

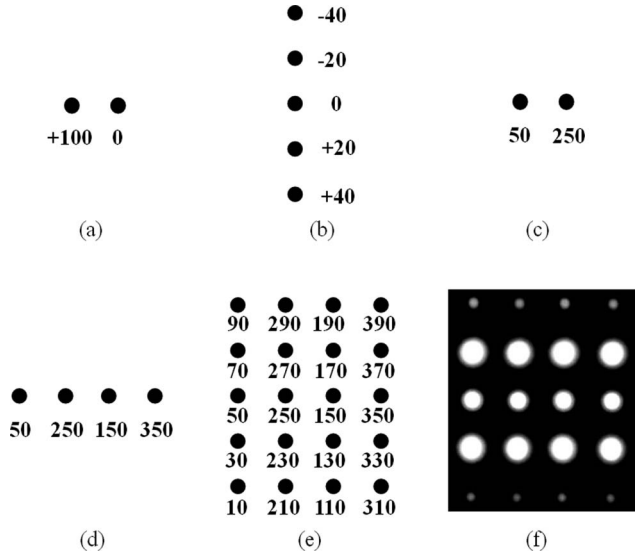

Fig. 1. Beam array with different frequency shifts: (a) frequency shifter in the Bragg regime; (b) Raman-Nath frequency shifter, (c) at position I in Fig. 2(a), (d) at position II in Fig. 2(a), (e) at position III in Fig. 2(a), and (f) real intensity distribution of 20 beams on a sensing card (all frequency shift values are with the unit of megahertz).

B. Bypass Cross Talk

In the proposed multibeam laser Doppler vibrometer, the interference of 20 object beams and one reference beam are detected by a high-speed photodetector. Besides the useful interference signals between the object beams and the reference beam, cross talk

between any two object beams also exists. Following are three methods to avoid the effect of cross talk during digital decoding in a 20-point LDV.

1. *By a Frequency Shift Higher Than Cross Talk*

For example, if the frequency shifts of 20 points are from 410 to 790 MHz with an interval of 20 MHz, the cross talk between any two object beams should be less than 400 MHz. Hence, it is possible to measure a Doppler frequency shift of ±10 MHz on each point, which is equivalent to ±7.75 m/s in velocity when a 1550 nm laser is used. However, in a digital decoding system, a higher sampling rate should be used to satisfy the Nyquist theorem, which implies high requirements on hardware. In addition, in order to achieve a high frequency resolution, the data to be processed should be longer. This will tremendously increase the processing time.

2. *By a Half-Step Frequency Shift*

Figure 1(e) shows the frequency shifts of 20 points, which are from 10 to 390 MHz with intervals of 20 MHz. Assuming the Doppler frequency shift on each point is within the range of ±3.3 MHz (equivalent to ±2.55 MHz in velocity when a 1550 nm laser is used), the vibration signals on different carriers are limited in the spectrum regions of 10 ± 3.3, 30 ± 3.3, …390 ± 3.3 MHz, and the cross-talk regions among 20 object beams are limited in the region of 20 ± 6.6, 40 ± 6.6, …380 ± 6.6 MHz. Hence, the necessary sampling rate and the data to be processed is only half that of the first method, but the same frequency resolution can be achieved. However, the velocity measurement range is only one-third of that in the previous method.

3. *By a High-Intensity Reference Beam and WFR Processing*

In this method, the frequency shifts are same as the second method. In Eq. (3), the intensity of the interference signals of the object beams and reference beam is determined by $\sqrt{I_R I_{O(i)}}$ ($i = 1,2,\ldots,20$), while the intensity of the cross talk between any two object beams is determined by $\sqrt{I_{O(m)} I_{O(n)}}$ ($m = 1, 2, \ldots 19$; $n = 2, 3, \ldots 20$; $m \neq n$). Once the intensity of the reference beam is much higher than the object beams, the useful interference signals will dominate the spectrogram. Hence, when a WFR or wavelet ridge method [22] is applied to detect the signals with the highest energy at a certain frequency range, it is still possible to retrieve the useful interference signals from the cross-talk region. Figure 3(a) shows the modulus (from 9 to 31 MHz) of a windowed Fourier transform of a signal captured in the proposed 20-point LDV. The gray scale indicates the signal energy at different frequencies. Signals at 10 and 30 MHz are obviously much higher than that at 20 MHz, where the largest cross-talk signal is found. Figure 3(b) shows the LabVIEW spectrum of the signal from 20-point LDV. The y axis shows the logarithmic value in decibels. A frequency comb containing 20 peaks is observed. Compared to the previous two methods, it has a large measurement range, the same as method 1, but only needs a low sampling rate, the same as method 2. However, as mentioned in Section 2, detecting a WFR or a wavelet ridge is also a time-consuming process.

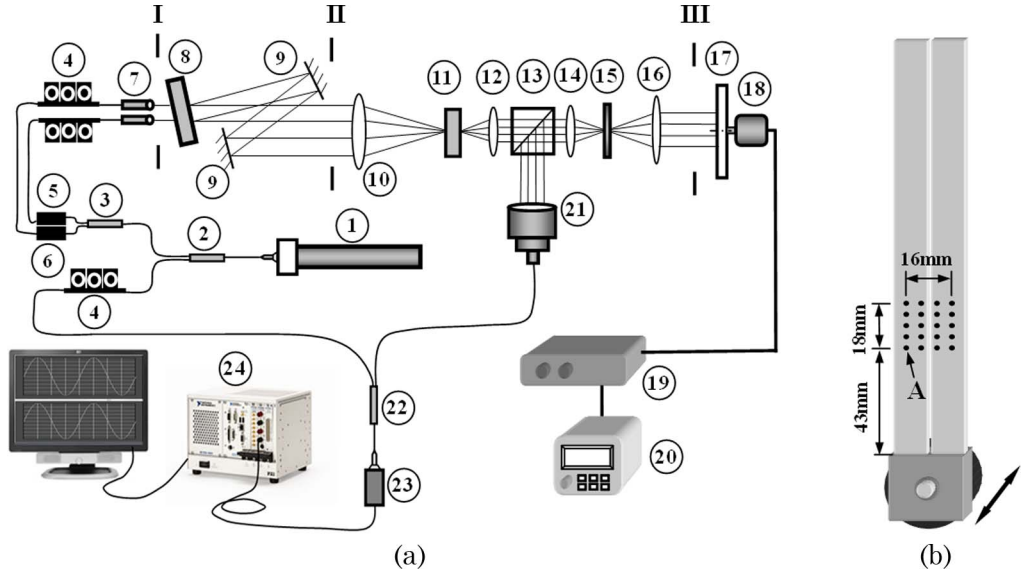

Fig. 2. (a) Top view of the experimental setup of the 20-beam laser Doppler vibrometer with a single detector. 1, 80 mW DFB laser system; 2, single-mode fiber coupler (1:99); 3, single-mode fiber coupler (20:80); 4, polarization controllers; 5, fiber-based AOM (250 MHz up-shift); 6, fiber-based AOM (50 MHz, up-shift); 7, GRIN lenses; 8, Bragg frequency shifter; 9, mirrors; 10, focusing lens; 11, Raman–Nath frequency shifter; 12, lens 1 to form a telescope system; 13, polarizing beam splitter; 14, lens 2 to form a telescope system; 15, quarter-wave plate; 16, imaging lens; 17, specimen; 18, shaker; 19, shaker controller; 20, function generator; 21, single-mode pigtailed collimator; 22, single-mode fiber coupler (30:70); 23, high-speed photodetector; 24, NI preamplifier and high-speed digitizer with processor. (b) Specimens: two cantilever beams with different thicknesses.

4. Experimental Illustration

Figure 2(a) shows the experimental setup of the proposed 20-point laser Doppler vibrometer. A DFB laser with a wavelength in the C-band (Photonik, 80 mW, $\lambda = 1548.53$ nm) is selected for its potential long-distance applications because a single-frequency high-power fiber laser in this wavelength is already available in the market. In addition, commercial telecom components, often with single-mode fiber technology, allow easily aligned and relatively cheap 1.5 μm systems [25]. The linearly polarized laser beam is split into a reference beam and an object beam. The object beam is then split into a 4 × 5 beam array by the frequency shifting system mentioned in Section 3 and collimated again by another lens before passing through a polarizing beam splitter (PBS). The polarization of the beams can be changed by a polarization controller so that most of the power can pass through the PBS. With another telescope system and a quarter-wave plate, the beam array is projected on a testing object with a retroreflective tape. The testing object is a pair of cantilever beams with different thicknesses that is excited by a shaker system whose frequency is controlled by a function generator. In this application, a 1300 Hz vibration is applied on the cantilever beams. Figure 2(b) shows the position and distribution of the projected beam array on the testing object. The reflected beam array is received by a large-beam fiber optic collimator (Princetel, CLF-155-28-FC, beam

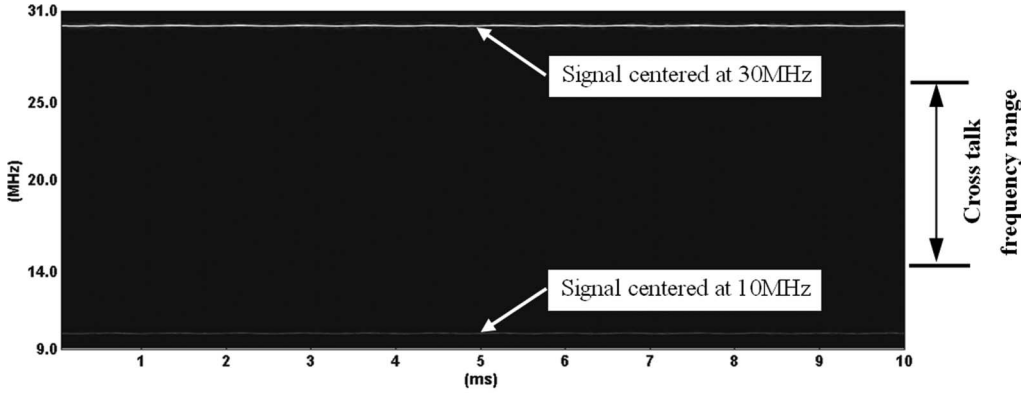

(a)

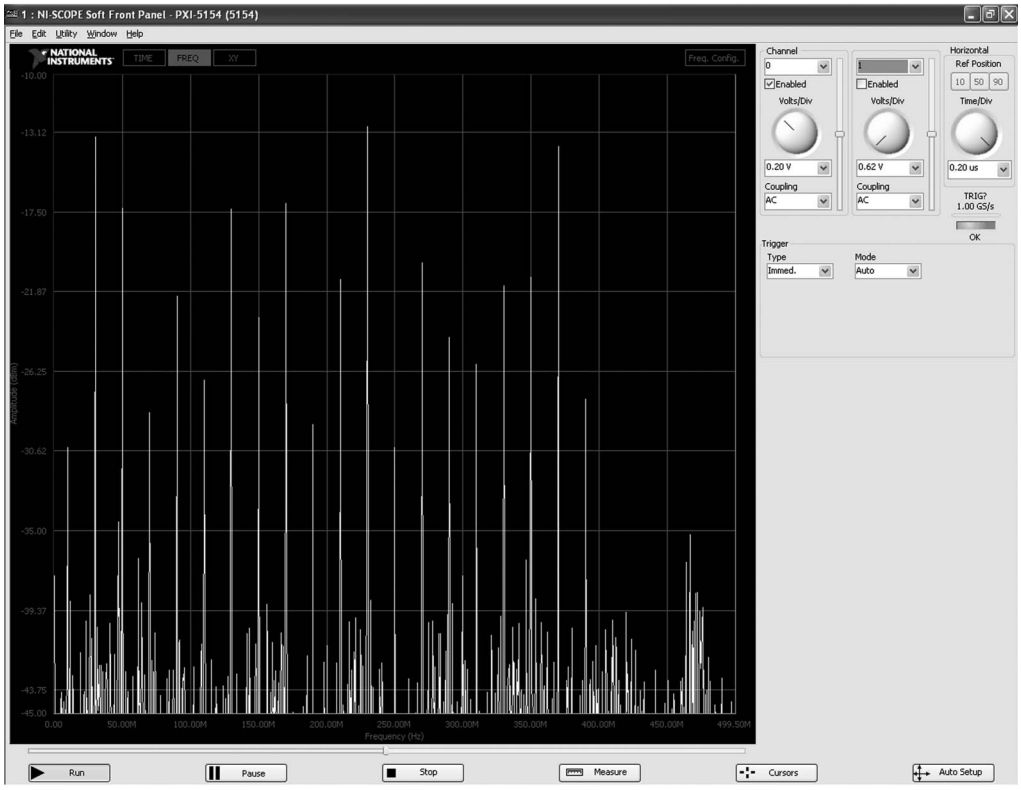

(b)

Fig. 3. (a) Spectrogram of detected signal in the frequency range from 9 to 31 MHz. (b) spectrum of the signal from the proposed 20-point LDV.

size 14 mm, focal length 75 mm, NA = 0.32). The object beams then interfered with a reference beam whose polarization is also adjusted to maximize the magnitude of the beating signal. The interference signal received by a high-speed indium gallium arsenide (InGaAs) photodetector (Thorlabs DET01CFC, 2 GHz) is amplified by a PXI preamplifier (National Instruments, PXI-5690, maximum 30 dB) and digitized by a high-speed A–D card (NI, PXI5154, 8 bit, 2 GS/s, 256 Mbytes on-board memory) with a rate of 1 G sampling points per second.

5. Results and Discussion

It is observed from Fig. 3(b) that the signal around 10 MHz has the lowest signal-to-noise ratio (SNR). This is reasonable because the power of the beam is one of the lowest and it is at the lower left corner of the beam array, so the coupling efficiency is relatively lower than other beams. The measurement results of this point [point A in Fig. 2(b)] are selected to present as they are expected to be the worst results among 20 points. Fourier analysis and WFR are applied to extract the velocity and displacement. Fourier analysis can directly extract the displacement that is proportional to the phase, and the velocity is obtained by a differentiation. The WFR method directly extracts the frequency fluctuation near the certain central frequency. Hence, the vibration velocity can be obtained directly, and the displacement can be obtained by integration. Figures 4(a) and 4(c) show the velocity and displacement obtained by WFR at point A, respectively. Figure 4(d) shows the displacement obtained by Fourier analysis, and Fig. 4(b) is the velocity after differentiation. A smoother velocity and displacement results are observed in WFR results, as a high efficiency on noise elimination is already proved by WFR. The measurement result is verified by a commercial single-point vibrometer. Figure 4(e) shows the displacement measurement on point A obtained by a Polytec PDV-100 vibrometer. An offset is observed as Figs. 4(c) and 4(d) show the relative displacement referring to the first measurement point, but this offset is removed in the measurement with the Polytec vibrometer. In addition, the phases are not exactly matching as these two measurements are not synchronized, but the amplitude and frequency obtained are almost the same. As Fig. 4 shows the results from a point (point A) with the lowest SNR, the results from the rest of the points are much better than that from point A.

Figure 5 shows the spectrograms of the signal around the central frequencies of 110, 130, 150, 170, and 190 MHz, respectively. The dashed curves are the WFRs of the signals at different frequency ranges. The frequency variations of the ridges are proportional to the velocities of the points on the third column, as shown in Fig. 1(e). A vibration node is observed near the third point as the vibration amplitude is almost zero, but increasing along both sides with opposite phase directions. Figure 6 is the three-dimensional (3-D) plot of the instantaneous

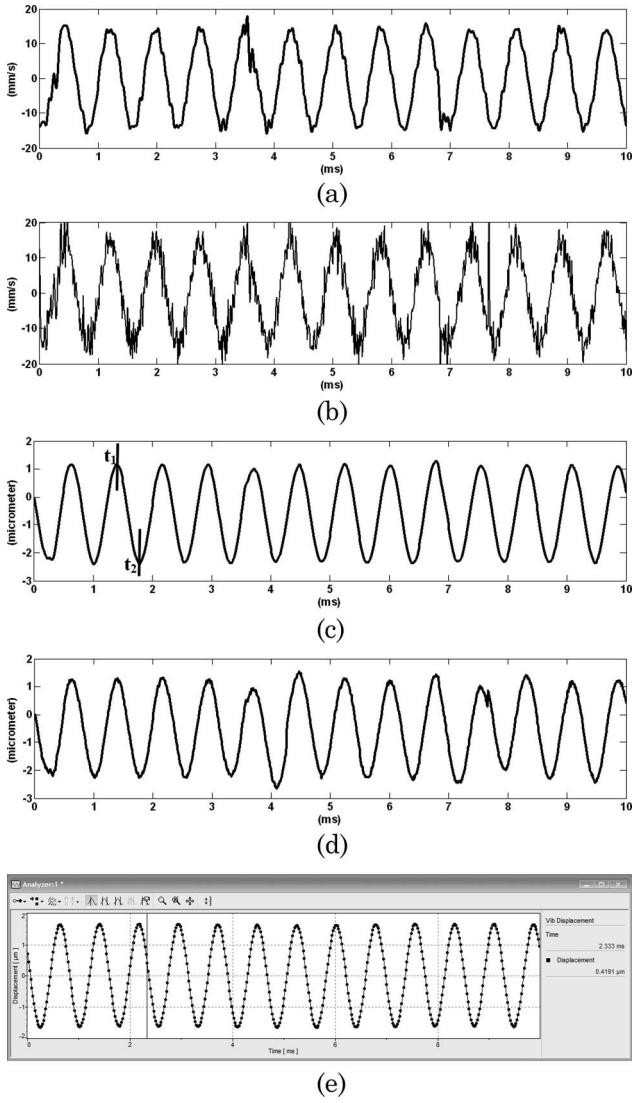

Fig. 4. Velocity of point A obtained (a) by the WFR method and (b) by Fourier analysis. The displacement of point A obtained (c) by the WFR method, (d) by Fourier analysis, and (e) by the Polytec PDV-100 single-point vibrometer.

displacements of two cantilever beams obtained by WFR at instants t_1 and t_2, as shown in Fig. 4(c). The mesh nodes represent the measurement points on two cantilever beams.

From the results presented above, vibration measurement on 20 points is executed by the proposed digital multibeam laser Doppler vibrometer with a signal detector. The sensitivity achieved is less than 50 nm with a wavelength of 1550 nm; the velocity range is more than ± 7.7 m/s when a suitable processing algorithm is selected. As the signal is detected by a high-speed photodetector and digitized by a high-speed A–D converter with a sampling rate of 1 GS/s, the vibration frequency to be measured can be more than 100 MHz. The on-board memory of the NI PXI5154 A–D card is 256 Mbytes. It can record an 8 bit signal with 0.25 s duration. Hence, the highest frequency resolution of this system is 4 Hz. Generally

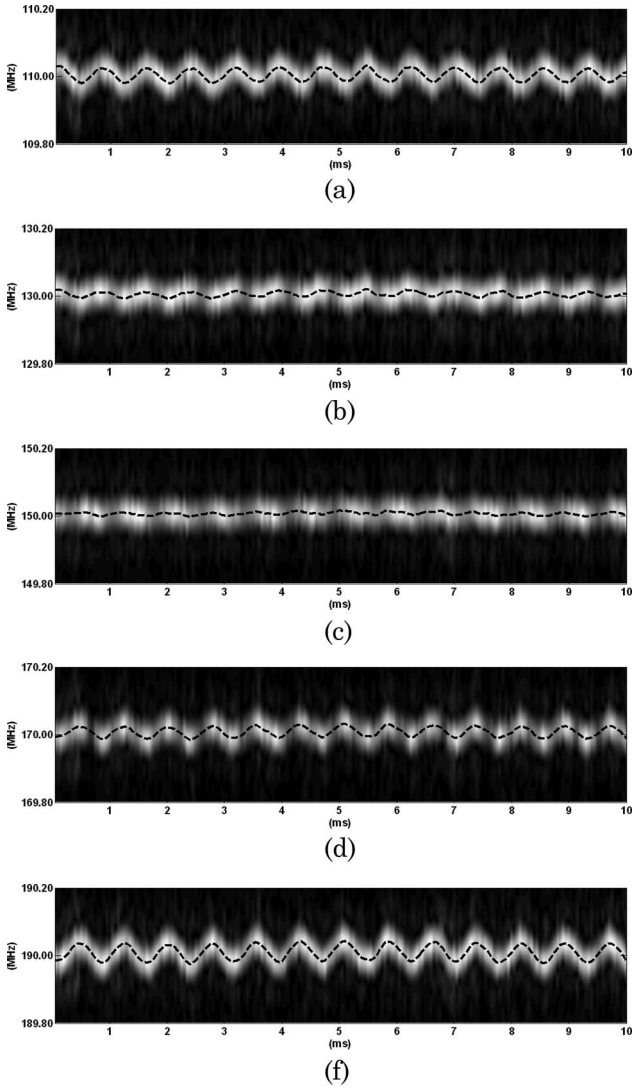

Fig. 5. Spectrogram of a signal at (a) 110, (b) 130, (c) 150, (d) 170, and (e) 190 MHz.

these specifications are enough for most applications in industrial area.

However, the system still has disadvantages and room for improvement in the following aspects. (1) The intensity of the beam array generated by the Raman–Nath frequency shifter is not uniform. In addition, the beams with lower intensity are found at the boundary. This will cause unbalanced SNR at different frequencies. Hence, a powerful laser source has to be used to satisfy the minimum SNR (in this application, >10 dB) of the beams with lower intensity. (2) The reflected beams may need a good mix before they are collected by a collimator. An improvement on the optical design for a proper mix may increase the coupling efficiency of the collimator. (3) With the proposed optical design, the position and angle of the receiving collimator still need fine adjustment to get 20 frequency peaks with high SNR simultaneously. (4) When a relatively high-intensity reference beam is used, it will introduce high noise in the low-frequency area, although, theoretically,

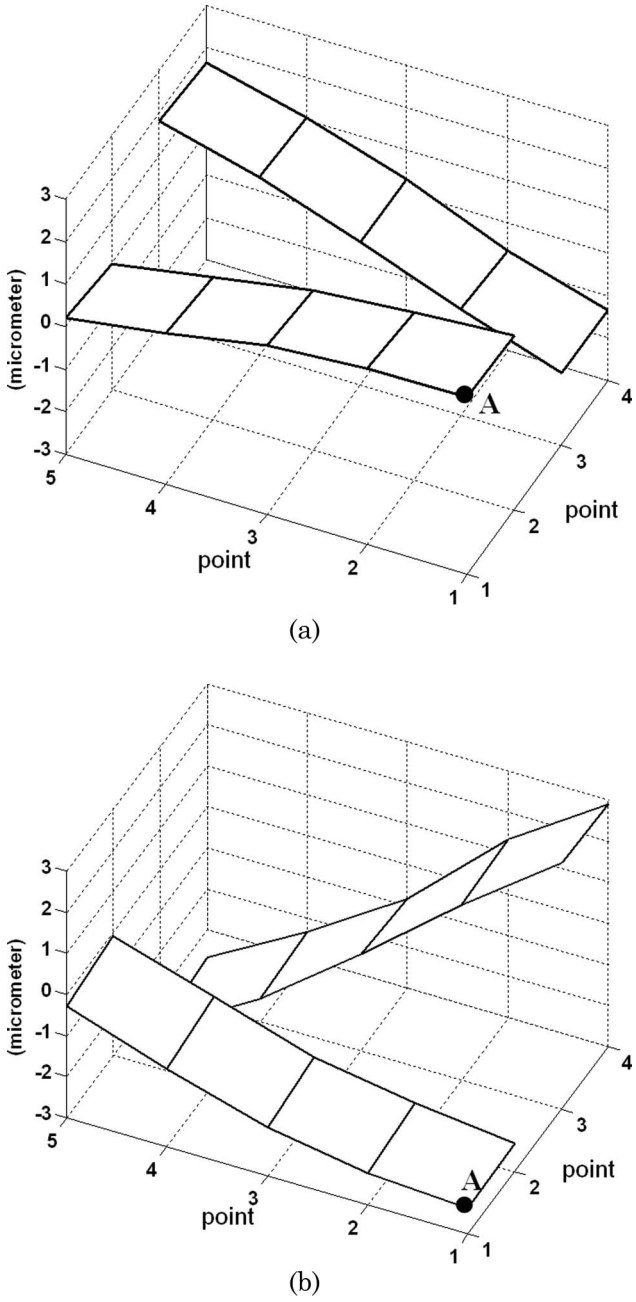

Fig. 6. 3-D plot of the instantaneous displacement of two cantilever beams at instants t_1 and t_2 as shown in Fig. 4(c).

the DC term is removed by the preamplifier. When a next-generation system is designed, it is better to avoid the low-frequency zone of <20 MHz. (5) Compared with our previous paper [20], the number of measurement points is doubled. It is still possible to increase the beam number and the measurement area. However, this will also increase the difficulties in collecting object beams into a single-mode fiber. In addition, higher requirements on hardware, such as a high sampling rate and a large sensor area are desired when the beam number increases. In the digital version, the processing time is long. Hence, real-time measurement is still difficult using a normal computer. Parallel computing might be an effective

way to reduce the processing time. (6) Once the velocity measurement range is increasing, the noise will be more serious, especially in an analog decoding system. In a digital version, the noise can be eliminated using different signal processing algorithms with the cost of longer processing time.

6. Concluding Remarks

In this paper, we proposed a 20-point laser Doppler vibrometer at a 1550 nm wavelength using a high-speed photodetector. Compared to a scanning laser Doppler vibrometer and multichannel LDV using detector arrays, the proposed technique has an advantage in simultaneous measurement of transient events with a relatively simple setup. Several methods to bypass the cross talk among object beams are discussed. Two typical signal processing algorithms are proposed to extract the velocity and displacement of a vibrating object. The results coincide with those from a commercial single-point LDV. The specifications of the proposed system can meet the requirements of most industrial applications. In addition, the concept can be extended to other technologies in laser Doppler metrology, such as laser Doppler velocimetry for in-plane measurement and laser Doppler microscopy for microcomponent measurements.

The authors thank Dr. K. Qian of the School of Computer Engineering, Nanyang Technological University for helpful discussions on signal processing algorithms.

References

1. P. Picart, J. Leval, D. Mounier, and S. Gougeon, "Time-averaged digital holography," Opt. Lett. **28**, 1900–1902 (2003).
2. P. Hariharan, B. F. Oreb, and C. H. Freund, "Stroboscopic holographic interferometry: measurements of vector components of a vibration," Appl. Opt. **26**, 3899–3903 (1987).
3. G. Pedrini, H. Tiziani, and Y. Zou, "Digital double pulse-TV-holography," Opt. Lasers Eng. **26**, 199–219 (1997).
4. J. M. Huntley, G. H. Kaufmann, and D. Kerr, "Phase-shifted dynamic speckle pattern interferometry at 1 kHz," Appl. Opt. **38**, 6556–6563 (1999).
5. G. H. Kaufmann and G. E. Galizzi, "Phase measurement in temporal speckle pattern interferometry: comparison between the phase-shifting and the Fourier transform methods," Appl. Opt. **41**, 7254–7263 (2002).
6. Y. Fu, G. Pedrini, and W. Osten, "Vibration measurement by temporal Fourier analyses of a digital hologram sequence," Appl. Opt. **46**, 5719–5727 (2007).
7. Y. Fu, R. M. Groves, G. Pedrini, and W. Osten, "Kinematic and deformation parameter measurement by spatiotemporal analysis of an interferogram sequence," Appl. Opt. **46**, 8645–8655 (2007).
8. P. Castellini, M. Martarelli, and E. P. Tomasini, "Laser Doppler vibrometry: development of advanced solutions answering to technology's needs," Mech. Syst. Signal Process. **20**, 1265–1285 (2006).
9. J. La, J. Choi, S. Wang, K. Kim, and K. Park, "Continuous scanning laser Doppler vibrometer for mode shape analysis," Opt. Eng. **42**, 730–737 (2003).
10. J. J. J. Dirckx, H. J. van Elburg, W. F. Decraemer, J. A. N. Buytaert, and J. A. Melkebeek, "Performance and testing of a four channel high-resolution heterodyne interferometer," Opt. Lasers Eng. **47**, 488–494 (2009).
11. A. Waz, P. R. Kaczmarek, M. P. Nikodem, and K. M. Abramski, "WDM optocommunication technology used for multipoint fibre vibrometry," Proc. SPIE **7098**, 70980E (2008).
12. W. Zheng, R. V. Kruzelecky, and R. Changkakoti, "Multichannel laser vibrometer and its applications," Proc. SPIE **3411**, 376–384 (1998).
13. R. Burgett, V. Aranchuk, J. Sabatier, and S. S. Bishop, "Demultiplexing multiple beam laser Doppler vibrometry for continuous scanning," Proc. SPIE **7303**, 730301 (2009).
14. J. M. Kilpatrick and V. Markov, "Matrix laser vibrometer for transient modal imaging and rapid non-destructive testing," Proc. SPIE **7098**, 709809 (2008).
15. R. Di Sante, "A novel fiber optic sensor for multiple and simultaneous measurement of vibration velocity," Rev. Sci. Instrum. **75**, 1953–1958 (2004).
16. K. Maru, K. Kobayashi, and Y. Fujii, "Multi-point differential laser Doppler velocimeter using arrayed waveguide gratings with small wavelength sensitivity," Opt. Express **18**, 301–308 (2010).
17. T. Pfister, L. Büttner, K. Shirai, and J. Czarske, "Monochromatic heterodyne fiber-optic profile sensor for spatially resolved velocity measurements with frequency division multiplexing," Appl. Opt. **44**, 2501–2510 (2005).
18. E. B. Li, J. Xi, J. F. Chicharo, J. Q. Yao, and D. Y. Yu, "Multipoint laser Doppler velocimeter," Opt. Commun. **245**, 309–313 (2005).
19. D. Garcia-Vizcaino, F. Dios, J. Recolons, A. Rodriguez, and A. Comeron, "One-wavelength two-component laser Doppler velocimeter system for surface displacement monitoring," Opt. Eng. **47**, 123606 (2008).
20. Y. Fu, M. Guo, and P. B. Phua, "Spatially encoded multibeam laser Doppler vibrometry using a single photodetector," Opt. Lett. **35**, 1356–1358 (2010).
21. G. Cloud, "Optical methods in experimental mechanics: Part 17: laser Doppler interferometry," Exp. Tech. **29**, 27–30 (2005).
22. S. Mallat, *A Wavelet Tour of Signal Processing* (Academic, 1998).
23. K. Qian, "Two-dimensional windowed Fourier transform for fringe pattern analysis: principles, applications and implementations," Opt. Lasers Eng. **45**, 304–317 (2007).
24. M. G. Moharam and L. Young, "Criterion for Bragg and Raman–Nath diffraction regimes," Appl. Opt. **17**, 1757–1759 (1978).
25. C. A. Hill, M. Harris, and K. D. Ridley, "Fiber-based 1.5 μm lidar vibrometer in pulsed and continuous modes," Appl. Opt. **46**, 4376–4385 (2007).